arXiv:1401.7450v1 [physics.soc-ph] 29 Jan 2014

Network Risk and Forecasting Power in Phase-Flipping Dynamical Networks

B. Podobnik,[1,2,3] A. Majdandzic,[1] C. Curme,[1] Z. Qiao,[4,5] W.-X. Zhou,[6] H. E. Stanley,[1] and B. Li[4,5,7]

[1] *Center for Polymer Studies and Department of Physics, Boston University, Boston, MA 02215, USA*
[2] *Faculty of Civil Engineering, University of Rijeka, 51000 Rijeka, Croatia*
[3] *Zagreb School of Economics and Management, 10000 Zagreb, Croatia*
[4] *NUS Graduate School for Integrative Sciences and Engineering, NUS, Singapore 117456, Singapore.*
[5] *Department of Physics and Center for Computational Science and Engineering, NUS, Singapore 117456, Singapore*
[6] *School of Business, School of Science, and Research Center for Econophysics, East China University of Science and Technology, Shanghai 200237, China*
[7] *School of Physics Science and Engineering, Tongji University, Shanghai, 200092, P R China*

In order to model volatile real-world network behavior, we analyze phase-flipping dynamical scale-free network in which nodes and links fail and recover. We investigate how stochasticity in a parameter governing the recovery process affects phase-flipping dynamics, and find the probability that no more than q% of nodes and links fail. We derive higher moments of the fractions of active nodes and active links, $f_n(t)$ and $f_\ell(t)$, and define two estimators to quantify the level of risk in a network. We find hysteresis in the correlations of $f_n(t)$ due to failures at the node level, and derive conditional probabilities for phase-flipping in networks. We apply our model to economic and traffic networks.

PACS numbers: 89.75.Hc, 64.60.ah, 05.10.-a,05.40.-a

Across a broad range of human activities—from medicine, weather, and traffic management to intelligence services and military operations—forecasting theories help us estimate the probability of future outcomes. In general, the greater the uncertainty of outcome, the more crucial that we be able to forcast future behavior. Since the nodes of many dynamic systems [1–21], such as traffic patterns and physiological networks, periodically fail and then recover—a disease spreads through an organism and then after a finite period of time the organism recovers—the forecasting power [22–24] is highly relevant—it allows us to estimate the probability of future node and link failure and recovery and to quantify the level of risk in any given dynamic network.

A recent paper details how the nodes in dynamic regular networks and Erdős Renyi networks (i) inherently fail, (ii) contiguously fail due to the failure of neighboring nodes, and (iii) recover [25]. These networks exhibit phase-flipping between "active" and "inactive" collective network modes. Here we analyze networks with highly heterogeneous degree distributions and we describe scale-free phase-flipping networks in which nodes and links fail and recover. We describe the collective behavior of these networks using two time-dependent network variables: the fraction of active nodes $f_n(t)$ and the fraction of active links $f_\ell(t)$. We place an emphasis on forecasting in dynamic networks—we want to calculate how many nodes will fail at any future time t—and quantify how risky networks are.

(i) At each time t any node in the system can independently fail, breaking its links with all other nodes, with a probability p. The internal failure state of node i we denote by spin $|s_i\rangle$ (if i is active, $|s_i\rangle = |1\rangle$).

(ii) The external failure states we denote by spin $|S_i\rangle$, where $|S_i\rangle$ is $|1\rangle$ if node i has more than T_h% active neighbors, and $|0\rangle$ (for a subsequent time $\tau' = 1$) with probability p_2 if $\leq T_h$ % of i's neighbors are active. For scale-free networks, a percentage threshold T_h is the more appropriate choice than the constant T_h used in Ref. [1, 25]. Node i—described by the two-spin state $|s_i, S_i\rangle$—is active only if both spins are up (1), i.e., if $|s_i, S_i\rangle = |1, 1\rangle$.

(iii) After a time period τ, the nodes recover from internal failure. Usually τ is random, but we also analyze the case when τ is constant [25].

Estimating how far the parameters of a dynamic system are from the area in parameter space characterized by high instability is crucial. For the network described in (i)–(iii) above, we arbitrarily choose parameters p_1 (related to p by $p_1 = 1 - \exp(-p\tau)$ [25]) and T_h. We then destabilize the network by increasing p_2, causing it to transition from phase I with predominantly active nodes to phase II with predominantly inactive nodes. In Fig. 1(a), for varying p_2, the first network statistic—the average $f_n(t)$, $\langle f_n\rangle$—gradually decreases for $p_2 \in (0, p_2')$ and then, at $p_2 \approx p_2'$, $\langle f_n\rangle$ shows a sudden network crash—a first-order phase transition. In Fig. 1(b) for $p_2 \in (0, p_2')$ the second network statistic—the standard deviation of $f_n(t)$, σ_n—becomes increasingly volatile. During network recovery, in Figs. 1(a) and 1(b) both $\langle f_n\rangle$ and σ_n follow a first-order phase transition, but at a value $p_2 = p_2''$, which differs from $(p_2 = p_2')$ obtained during the I–II transition. Because $\langle f_n\rangle$ and σ_n are dependent upon the initial node spins in the network, $p_2' \neq p_2''$ implies the existence of hysteresis [26–29]. To estimate the part of the (p_1, p_2) phase space that is unstable, we calculate the discontinuity (p_2', p_2'') values for varying p_1 values [see

Fig. 1(b)]. Figure 1(c) shows a hysteresis with two discontinuity lines (spinodals) in the (p_1, p_2) space. The closer the (p_1, p_2) of a network is to the left spinodal in Fig. 1(c), the less stable the network.

Reference [25] reports that introducing both a dynamic recovery with a (constant) parameter ($\tau \neq 0$) and a stochastic contiguous spreading ($p_2 \neq 1$) leads to spontaneous collective network phase-flipping phenomena. Figure 1(d) shows the fraction of active nodes $f_n(t)$ for constant τ ($\Delta\tau = 0$) that corresponds to the volatile state X_A shown in Fig. 1(c). Figure 1(d) shows that if τ is not constant but a random variable from a homogeneous probability distribution function (pdf), the phase-flipping phenomenon and thus the collective network mode disappears with increasing $\Delta\tau$ (increasing stochasticity in τ). Beginning with the relation $p_1 = 1 - \exp(-p\tau)$ [25] when τ is constant, we confirm this result. Suppose a network is initially set at a phase-flipping state X_A [Fig. 1(c)]. If τ follows a homogeneous pdf, $H(\tau_0 - \Delta\tau, \tau_0 + \Delta\tau)$, we easily derive the average parameter $p_1^* \equiv p_1(\Delta\tau)$ as

$$E(p_1^*) = 1 - \exp(-p\tau_0)\sinh(p\Delta\tau)/p\Delta\tau, \qquad (1)$$

and the average deviation of p_1^* from $p_1 \equiv p_1(\Delta\tau = 0)$, $E(p_1^*) - p_1 = \exp(-p\tau_0)[1 - \sinh(p\Delta\tau)/p\Delta\tau] < 0$. With increasing $\Delta\tau$, $E(p_1^*) - p_1$ decreases and $E(p_1^*)$ moves

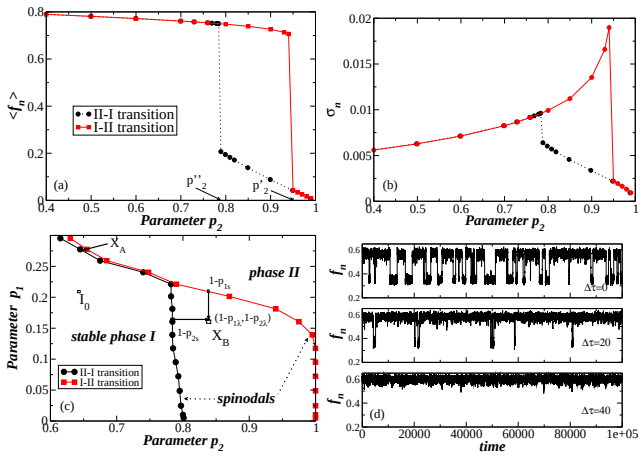

FIG. 1: Network statistics used in analyzing (in)stability in the (i)–(iii) networks. In (a)–(c) we start with a BA network with $N = 10,000$ and $\langle k \rangle = 3$, and then introduce the (i)–(iii) network, where $T_h = 50\%$ and $\tau = 50$. Fixing p_1 and increasing p_2, for each (p_1, p_2) we calculate the fraction of active nodes, $f_n(t)$. We show hystereses for two network statistics: (a) the average $f_n(t)$, $\langle f_n \rangle$, and (b) the standard deviation of $f_n(t)$, σ_n. We use $p_1 = 0.2$ ($p = 0.004$) in two directions: from $p_2 = 0$ to $p_2 = 1$, and then from $p_2 = 1$ to $p_2 = 0$. As $p_2 \to p_2'$, $\langle f_n \rangle$ and σ_n exhibit first-order transitions. (c) Emergence of hysteresis in (p_1, p_2) space. The hysteresis point X_A is characterized by $\tau = 50$, $p = 0.0065$ ($p_1 = 0.277$), and $p_2 = 0.65$. (d) If τ is a random variable from a homogeneous pdf, $H(\tau_0 - \Delta\tau, \tau_0 + \Delta\tau)$, with $\tau_0 = 50$, the phase-flipping phenomenon gradually dissappears with increasing $\Delta\tau$.

from a volatile network regime (X_A) to a more stable network regime. Hence at X_A the less dispersed τ is (and also p_1), the more pronounced the phase-flipping. Hereafter, we analyze networks with constant τ.

We next explore the diagnostic and forecasting power of dynamic networks. When internal (X) and external (Y) failures are independent, according to probability theory $P(X \cup Y) = P(X) + P(Y) - P(X)P(Y)$, from which Ref. [25] calculates the probability $a = a(p, p_2, T_h) \equiv P(X \cup Y)$ that a randomly chosen node i is inactive

$$a = p + p_2(1-p)\Sigma_k P(k)E(k, m, a), \qquad (2)$$

equal to the fraction of inactive nodes, $a = 1 - \langle f_n \rangle$. Clearly, the internal and external failures are only approximately independent [25]. Here $P(k)$ is the degree distribution, T_h, p, and p_2 are described in (i)–(ii) above, $m \equiv T_h k$, $E(k, m, a) \equiv \Sigma_{j=0}^{m} a^{k-j}(1-a)^j \binom{k}{k-j}$ is the probability that the neighborhood of node i is critically damaged. For a network with N nodes, each with probability $(1-a)$ of being active, using a binomial distribution we obtain any moment of f_n of order q,

$$\langle f_n^q \rangle \equiv \Sigma_{j=0}^{N} (\frac{j}{N})^q a^{N-j}(1-a)^j \binom{N}{j}, \qquad (3)$$

that is, for large values of N, $\langle f_n^q \rangle \approx \int dx x^q G(x, \mu = 1-a, \sigma = \sqrt{a(1-a)/N})$—G stands for Gaussian. The dependence of f_n^q on a explains why both $\langle f_n \rangle$ and σ_n in Fig. 1 show discontinuities for the same p_2 values.

We next use the diagnostic power of the (i)-(iii) network to quantify the level of its stability. Using the first two moments of Eq. (3), we define network risk (volatility) as $\sigma_n \equiv \sqrt{\langle f_n^2 \rangle - (\langle f_n \rangle)^2}$. Because a network is more stable when $f_n(t)$ is less volatile ($\sigma_n \to 0$) and when $\langle f_n \rangle$ is as close to 1 as possible, we propose another network stability measure, the stability network ratio,

$$\langle f_n \rangle / \sigma_n, \qquad (4)$$

where the larger the ratio, the more stable the network. Figure 2(a) shows that for a (i)–(iii) network the ratio exhibits hysteresis behavior, e.g., with increasing instability ($p_2 \to 1$), $\langle f_n \rangle / \sigma_n$ decreases. When N is large, $\langle f_n \rangle / \sigma_n = \sqrt{(1-a)N/a}$ [see Eq. (3)]. In practice, if two networks have equal $\langle f_n \rangle$, but different σ_n, the one with the larger ratio is more stable. Note that a similar first-to-second moment of a price return is proposed in finance to quantify the performance of a financial asset [30]. Similar signal-to-noise ratio defined as the ratio of mean to standard deviation of a signal is used widely in science and engineering [31].

In addition to estimating network volatility, we also need to forecast, having the initial configuration of active nodes, how many nodes will have failed at any future time t. We allow the (i)–(iii) network in Fig. 1(c),

initally at stable state I_0, to move δ steps (with p_1 changing linearly) to a highly volatile phase-flipping state X_A. Figure 2(b) shows a representative $f_n(t)$. We always start from the same initial I_0, perform a large number of simulations [see Fig. 2(c)], and obtain the conditional distribution function (cdf), $C(f_n)$, from which we calculate the probability ($\int_{0.01q}^{1} C(f_n)df_n$) that no more than $q\%$ nodes will be inactive at $t = 2\delta$. In finance, this probability approximates the risk that a substantial fraction of financial system will collapse, the so-called "systemic risk" [32].

When we use f_n we are assuming that every node is equally important. This frequently does not hold for real-world networks [2, 3, 33], e.g., when large banks become dysfunctional they affect the overall financial network much more than dysfunctioning small banks. In the (i)–(iii) network the importance of each node is governed by network topology—the time-dependent node degree, $k(t)$. A randomly chosen link is active if both its nodes are active and so the probability that the link is active is $(1-a)^2$. The average number of active links is

$$\langle L\rangle = (1-a)^2 L_T, \tag{5}$$

where $L_T \equiv 1/2\Sigma_{i=1}^{N} k_i$ denotes the total number of links

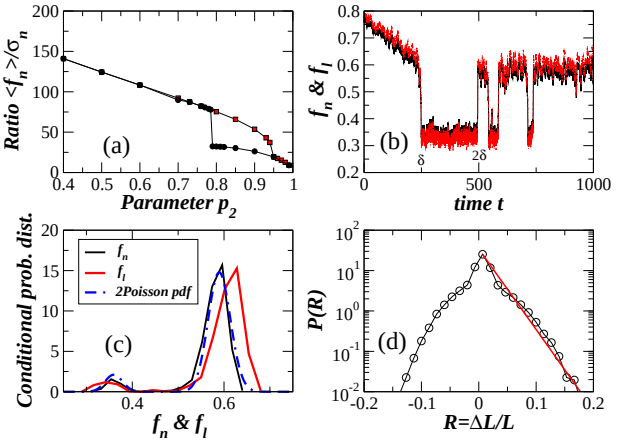

FIG. 2: Network estimator and forecasting in the (i)-(iii) networks. (a) Network estimator, the ratio $\langle f_n\rangle/\sigma_n$, exhibits a strong hysteresis—the larger $\langle f_n\rangle/\sigma_n$, the more stable the network. The parameters used are as those in Fig. 1(a). (b) The two fractions, f_n and f_ℓ, of the network with time-dependent p_1 that moves from I_0 (Fig. 1(c)) at time $t = 0$ to X_A during the first $\delta = 250$ steps. From δ to 2δ, the network stays in X_A. Upon reaching X_A, the network phase-flips between mainly "active", I, and mainly "inactive" phases, II. (c) Moving from I_0 to X_A after $t = 2\delta$ we calculate two *cdf*s, $C(f_n)$ and $C(f_\ell)$, both exhibiting a highly asymmetric bimodal shape. From $C(f_n)$ we can estimate the percentage of (in)active nodes at future t. Shown also is a combination of two Poissonian distributions, $w_1P(\lambda_1) + w_1P(\lambda_2)$ where $w_1 = 0.1$, $w_2 = 0.9$, $\lambda_1 = 0.59$ and $\lambda_2 = 0.36$, where λ_1 and λ_2 are $\langle f_n\rangle$ values in I and II. (d) For the number of active links, $L(t)$, we show $P(\Delta L(t)/L(t))$, and its exponential fit.

when all links are active. Similar to Eq. (3) for a network with L_T links, each with probability $u \equiv (1-a)^2$ of being active, a $q-$order moment of $f_\ell(t) = L(t)/L_T$—the fraction of active links—is

$$\langle f_\ell^q\rangle \equiv \Sigma_{j=0}^{L_T}(\frac{j}{L_T})^q u^j(1-u)^{L_T-j}\binom{L_T}{j}. \tag{6}$$

Figure 2(b) shows a representative $f_\ell(t)$, and Fig. 2(c) shows $C(f_\ell)$ (broader than $C(f_n)$) from which we can calculate the probability ($\int_{0.01q}^{1} C(f_\ell)df_\ell$) that no more than $q\%$ of links will be inactive at t. Figure 2(d) shows the pdf of the relative change in $L(t)$ and its exponential fit—which is potentially important information for network management. Note that $\mathcal{L}(t) = L_T[1 - f_\ell(t)]$ denotes the loss of a network's links. Using Eq. (5) we obtain $\langle\mathcal{L}\rangle \equiv L_T - \langle L\rangle = a(2-a)L_T$.

The (i)–(iii) network model offers one more potentially important forecasting property. Suppose a network set in a state X_B (see Fig. 1(c)) within the hysteresis regime is predominantly inactive. Reference [25] defines a local time-dependent parameter $p_{2,\lambda}(t) = \frac{1}{\lambda}\Sigma_{i=1}^{\lambda} p_2(t+1-i)$ as the average fraction of externally failed nodes over the most recent interval of length λ. When $p_{2,\lambda}(t)$ crosses the "left" spinodal, the network shifts from the inactive phase II to the active phase I. Similarly, $p_{1,\lambda}(t) = \frac{1}{\lambda}\Sigma_{i=1}^{\lambda} p_1(t+1-i)$. In Ref. [25] the pdf of $p_{2,\lambda}(t)$ ($p_{1,\lambda}(t)$) determines the average lifetime of the system in I and II. Here we find that $p_2(t)$ follows a binomial distribution that can be approximated for large samples n with the normal distribution $N(\mu = p_2, \sigma^2 = p_2(1-p_2)/n) \equiv P(p_2(t)) \sim \exp[-\frac{n(p_2(t)-p_2)^2}{2p_2(1-p_2)}]$, where $n = NE(a(p_1,p_2),k,m)$ [see Eq. (2)]. From $p_{2,\lambda}(t) = \frac{1}{\lambda}\Sigma_{i=1}^{\lambda} p_{2,t+1-i}$ we easily derive $p_{2,\lambda}(t) = p_2(t)/\lambda + p_{2,\lambda}(t-1) - p_2(t-\lambda)/\lambda$.

Thus, having information about the previous $p_{2,\lambda}$, $p_{2,\lambda}(t-1)$, we can forecast the current value, where the

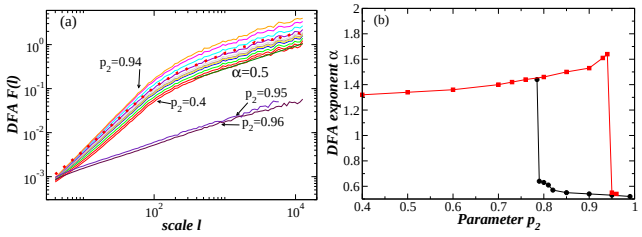

FIG. 3: Emergence of correlations at the network level due to failure at the node level. (a) For each time series (constant p_2) used in Fig. 1(a), we show the DFA plot of $f_n(t)$ vs. scale ℓ, $F(\ell) \propto (\ell)^\alpha$ for the I-II transition. With increasing p_2 up to 0.94, $F(\ell)$ moves upward, accompanied by small (b) increase in the DFA exponent α—α exhibits a cross-over at a scale l that varies with the recovery times τ and τ'. Suddenly, at $p_2 \approx 0.94$, the DFA exponent drops in a first-order phase transition. We also show correlations in the fraction of externally failed nodes (dotted lines), responsible for correlations in f_n. (b) Exponent α, calculated for both I-II and II-I transitions for scales $\ell \leq 100$, exhibits a clear hysteresis.

closer $p_{2,\lambda}$ is to a spinodal, the larger the probability that the phase will flip. We quantify this probability using the conditional distribution function (cdf) $C(p_{2,\lambda}(t)) \sim \exp[-\frac{N\lambda^2 E(a(p_1,p_2),k,m)(p_{2,\lambda}(t)-p_{2\lambda}(t-1)+p_2(t-\lambda)/\lambda-p_2/\lambda)^2}{2p_2(1-p_2)}]$. This probability can be used to estimate, given the most recent local state $p_{2\lambda}(t-1)$ and $p_2(t-\lambda)$, the probability $P(x \leq p_{2s}|p_{2\lambda}(t-1), p_2(t-\lambda))$ that the network will move from being predominantly inactive, II, to predominantly active, I—here, as in [25], p_{2s} is a spinodal value where the network phase-flips from II to I [Fig. 1(c)]. Similarly, if p_{1s} defines a spinodal value at which the network phase-flips from phase I to II [Fig. 1(c)], from the cdf $C(p_{1\lambda}(t)) \sim \exp[-\frac{N\lambda^2(p_{1,\lambda}(t)-p_{1\lambda}(t-1)+p_1(t-\lambda)/\lambda-p_1/\lambda)^2}{2p_1(1-p_1)}]$ we can estimate the probability $P(x \geq p_{1s}|p_{1\lambda}(t-1), p_1(t-\lambda))$ that the network will fall into the mainly inactive phase (e.g., as in an economic recession) within the next period.

Finally we examine the emerging hysteresis in correlations of $f_n(t)$ due to network dysfunctionality at the node level. For each time series $f_n(t)$ ($\tau =$ const) in Figs. 1(a) and 1(b) we apply detrended fluctuation analysis (DFA) [34]—$F^2(l) \propto l^{2\alpha}$. Figure 3(a) shows that $f_n(t)$ exhibits finite-range correlations of the random-walk type ($\alpha \approx 1.5$) with a clear first-order phase transition, in which a sudden change in the correlation exponent α occurs when p_2 approaches the value at which we expect network collapse (see Fig. 1). An approximate explanation of the correlations in $f_n(t)$ is that correlations in $f_n(t)$ and its hysteresis behavior are due to correlations in the fractions of externally failed nodes $p_2(t)$ and internally failed nodes $p_1(t)$. Figure 3(a) confirms this assumption by showing only correlations in $p_2(t)$. The existence of hysteresis [27–29] in Fig. 3(b) indicates that the correlations in collective modes are not the same when the network approaches network collapse and when the network recovers—if, e.g., our network models the global economy, then when the economy moves from "bad" to "good" years, "good" years are never as good as the previous "good" years.

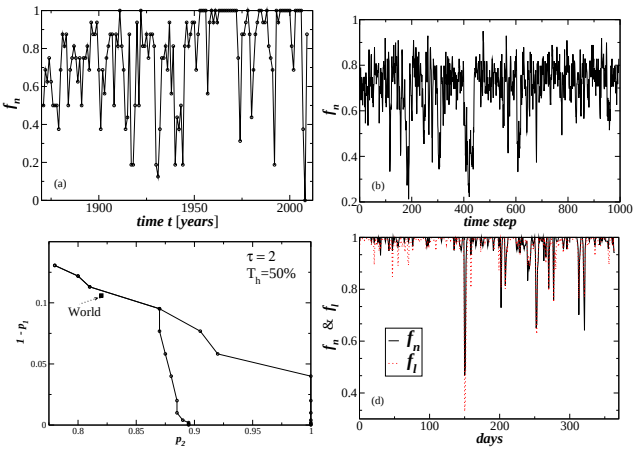

FIG. 4: Application of dynamical networks. (a) Economics—how far is an economy from a volatile regime? Fraction of developed countries, $f_n(t)$, not in recession ($\Delta gdp > 0$). (b) For a (i)-(iii) network we show the model's $f_n(t)$ obtained by fitting the first and the second moments in (a), where $\tau = 1.3$, $T_h = 56$ %, $p_1 = 0.103$ and $p_2 = 0.77$. (c) Hysteresis with two spinodals for the (i)-(iii) network with $N = 100$, $\tau = 2$, and $T_h = 50$ %. The parameter set is close to the critical line in the supercritical region. (d) Air traffic network. Fraction of active Northeastern US airports, f_n, with more than 40% of canceled flights. We also show f_ℓ.

To demonstrate the utility of the (i)–(iii) network model when analyzing real-world networks, we first analyze a small economic network of 19 developed countries [35], and use an output measurement of trading dynamics, *per capita* gross domestic product—*gdp*. For each country and for each year t between 1870 and 2012 [36], a country (node) is active if the *gdp* growth is non-negative (if it has been a "good" year). Figure 4(a) shows the fraction of active countries $f_n(t)$ that are becoming increasingly interdependent due to globalization [the non-stationary analyzed in Fig. 2(b)]. When we disregard this non-stationarity we find model parameters ($p = 0.082 \pm 0.02$, $p_2 = 0.77 \pm 0.03$, $\tau = 1.33 \pm 0.5$, and $T_h = 56 \pm 3\%$) for which the $\langle f_n \rangle$ of our model and the second network moment σ_n best fit the empirical moments. Figure 4(b) shows the $f_n(t)$ of the model. From $p_1 = 1 - \exp(-p\tau)$ [25], $p_1 = 0.103$ suggests that any randomly chosen developed country will experience recession (failure) approximately every ten years, since p_1 represents the average fraction of internally failed nodes [25]. The parameter $p_2 = 0.77$ means that there is an $\approx 77\%$ probability that a country will undergo recession if its trading partners have recently experienced recession. Figure 4(c) shows the hysteresis [27] in (p_1, p_2) space for the (i)–(iii) network model with $\tau = 2$ and $T_h = 50\%$. We find that developed countries with $p_1 = 0.106 \pm 0.01$, $p_2 = 0.82 \pm 0.02$ lie close to a critical hysteresis line–an indication that the world economy is highly unstable. We next analyze $f_n(t)$ for 23 Latin American countries, 25 EU countries, and 25 Asian countries for each year since 1980. We calculate the network stability ratio $\langle f_n \rangle / \sigma_n$ of Eq. (4) for each group and obtain the values 3.25, 4.15, and 6.95, implying that Asian countries are best performers.

We next analyze the airport traffic network [37] in the Northeastern United States (The Library of Congress definition) comprising 66 airports (nodes), and we consider only those flights (links) within the Northeast. For each day during the period 6/1/2012 – 5/31/2013 we calculate the fraction of failed airports $1 - f_n(t)$. We arbitrarily define failed airports as those in which more than $T_h = 40\%$ flights have been canceled for the day. The air traffic network in Fig. 4(d) shows a much higher level of nodes's stability than is typical of economic networks—rarely does $1 - f_n(t)$ drop to 40%. Since air traffic

network is known to be scale-free [22], we apply the (i)–(iii) network model to fit the empirical $\langle f_n \rangle$ and σ_n data to the models's parameters—$p = 0.011 \pm 0.003$ and $p_2 = 0.92 \pm 0.03$. Note that in air traffic network although it is common for links to fail (for flights to be canceled), airports still function properly. This implies that the (i)–(iii) dynamic network model could be extended to introduce item (iv), the probability, p_3, that each link can fail.

BP thanks the support of ZSEM (Grant ZSEM08007). This work is also partially supported by an NUS Grant "Econophysics and Complex Network" (R-144-000-313-133). The BU work is supported by NSF (Grant CMMI 1125290).

[1] D. J. Watts and S. H. Strogatz, Nature **393**, 440 (1998).
[2] R. Albert and A. -L. Barabási. Rev. Mod. Phys. **74**, 47 (2002).
[3] S. N. Dorogotsev and A. V. Goltsev, Rev. Mod. Phys. **80**, 1275 (2008).
[4] M. E. J. Newman, Networks: An Introduction. (Oxford Univ. Press, 2010).
[5] P. Holme and J. Saramaki, Phys. Reports **519**, 97 (2012).
[6] N. Pierra, B. Goncalves, R. Pastor-Satorras and A. Vespignani, Sci. Rep. **2**, 469 (2012).
[7] A. -L. Barabási and R. Albert, Science **286**, 509 (1999).
[8] S. N. Dorogovtsev, J. F. F. Mendes, and A. N. Samukhin, Phys. Rev. Lett. **85**, 4633 (2000).
[9] P. L. Krapivski, S. Redner, and F. Leyraz, Phys. Rev. Lett. **85** 4629 (2000).
[10] A. Krawiecki, J. A. Holyst, and D. Helbing, Phys. Rev. Lett. **89**, 158701 (2002).
[11] R. Pastor-Satorras and A. Vespignani, Phys. Rev. Lett. **86**, 3200 (2001).
[12] L. Adamic and B. A. Huberman, Nature **401**, 131 (1999).
[13] R. Albert, H. Jeong, and A. L. Barabási, *ibid.* **406**, 378 (2000).
[14] R. Milo *et al.* Science **298**, 824 (2002).
[15] D. Garlaschelli, G. Caldarelli, and L. Pietronero, Nature **423**, 165 (2003).
[16] S. V. Buldyrev *et al*, Nature **464**, 1025 (2010).
[17] R. Cohen, K. Erez, D. ben-Avraham, S. Havlin, Phys. Rev. Lett. **85**, 4626 (2000).
[18] R. Parshani, S. V. Buldyrev, and S. Havlin, Proc. Natl. Acad. Sci. USA **108**, 1007 (2011).
[19] N. Perra *et al.*, Phys. Rev. Lett. **109**, 238701, (2012).
[20] J. Gao, S. V. Buldyrev, H. E. Stanley, and S. Havlin, Nature Physics **8**, 40 (2012).
[21] B. Podobnik, M. Dickison, D. Horvatic, and H. E. Stanley, Europhys. Lett. **100**, 50004 (2012).
[22] V. Colizza, A. Barrat, M. Barthelemy, and A. Vespignani. Proc. Natl. Acad. Sci. USA **103**, (2005).
[23] A. Vespignani, Science **325**, 425 (2009).
[24] M. Kolar, L. Song, A. Ahmed, and E. P. Xing, The Annals of Applied Statistics **4**, 94 (2010).
[25] A. Majdandzic *et al.*, Nature Physics, **10**, 34 (2014).
[26] T. A. Kesselring *et al.*, Scientific Reports **2**, 474 (2012).
[27] O. J. Blanchard and L. H. Summers, European Economic Review **31**, 288 (1987).
[28] D. Angeli, J. E. Jr. Ferrell, and E. D. Sontag, Proc. Natl. Acad. Sci. USA **17**, 1822 (2004).
[29] J. Das *et al.*, Cell **136**, 337 (2009).
[30] W. F. Sharpe, Journal of Business **39**, 119 (1966).
[31] J. T. Bushberg *et al.*, The Essential Physics of Medical Imaging. (Lippincott Williams & Wilkins, 2006).
[32] D. Bisias, M. Flood, A. W. Lo, and S. Valavanis, Working Paper 0001 (2012).
[33] W. Miura, H. Takayasu, and M. Takayasu, Phys. Rev. Lett. **108**, 168701 (2012).
[34] C. K. Peng *et al*, Phys. Rev. E **49**, 1685 (1994).
[35] The dataset includes 15 EU countries, the USA, Australia, New Zealand, and Canada.
[36] http://www.ggdc.net/maddison/maddison-project/home.htm
[37] http://www.rita.dot.gov/bts/